

Cortical hyperexcitability and sensitivity to discomfort glare

Gary Bargary^{a,*}, Michele Furlan^b, Peter J. Raynham^c, John L. Barbur^a, Andrew T. Smith^b^a Applied Vision Research Centre, School of Health Sciences, City University London, Northampton Square, London EC1V 0HB, UK^b Department of Psychology, Royal Holloway University of London, Egham Hill, Egham TW20 0EX, UK^c The UCL Institute for Environmental Design and Engineering, University College London, Gower Street, London WC1E 6BT, UK

ARTICLE INFO

Article history:

Received 25 November 2014

Received in revised form

16 January 2015

Accepted 4 February 2015

Available online 7 February 2015

ABSTRACT

It is well established that there are two main aspects to glare, the visual impairment and the discomfort, known as disability and discomfort glare, respectively. In contrast to the case of disability glare we understand very little about the underlying mechanisms or physiology of discomfort glare. This study attempts to elucidate the neural mechanisms involved using fMRI and glare sources with controlled levels of retinal illuminance. Prior to carrying out the fMRI experiment, we determined each participant's discomfort glare threshold. The participants were then divided into two groups of equal size based on their ranked sensitivity to discomfort glare, a low and high sensitivity group. In the fMRI experiment each participant was presented with three levels of glare intensity whilst simultaneously required to carry out a simple behavioral task. We compared BOLD responses between the two groups and found that the group more sensitive to glare had an increased response that was localized at three discrete, bilateral cortical locations: one in the cuneus, one in the lingual gyri and one in the superior parietal lobules. This increased response was present for all light levels tested, whether or not they were intense enough to cause discomfort glare. Based on the results, we present the case that discomfort glare may be a response to hyperexcitability or saturation of visual neurons.

© 2015 The Authors. Published by Elsevier Ltd. This is an open access article under the CC BY license (<http://creativecommons.org/licenses/by/4.0/>).

1. Introduction

Glare, as commonly understood, is a phenomenon whereby a bright light source can cause a debilitating effect on the observer. The first systematic investigations into glare began by recognizing that both visual disability and discomfort can be experienced in the presence of bright sources of light. Since the methods available to quantify disability and discomfort were quite different, the various studies evolved into two, relatively independent research areas (Stiles, 1929b). One branch of research, known as disability glare, examined how a bright source can affect the visibility of other objects in the visual field (Holladay, 1926; Stiles, 1929a), while the other, known as discomfort glare, focused on the discomfort or distraction element experienced by the observer (Luckiesh and Holladay, 1925). The division of labor proved very successful in understanding disability glare as it allowed researchers to focus solely on retinal image changes caused by scattered light and the corresponding effects on visual performance. This led to accurate models of how light is scattered in the eye, consequently reducing the contrast of the retinal image (Stiles, 1929c; van den Berg and Franssen et al., 2013; Vos, 2003a).

The progress made in discomfort glare has been less satisfactory; although some advances have been made in predicting how uncomfortable a given lighting installation might be (Vos, 1999, 2003b), the mechanisms for discomfort glare and the corresponding physiological underpinnings remain largely unexplained.

Most studies on discomfort glare have focused on photometric properties of the glare source (Hopkinson, 1957; Luckiesh and Guth, 1949; Luckiesh and Holladay, 1925; Vermeulen and de Boer, 1952), and the results have led to improvements in discomfort glare metrics for the lighting industry (CIE, 1995; Vos, 1999). The few studies that have considered physiological correlates of discomfort have focused mainly on its efferent manifestations. Early work, for example, was concerned with pupil size fluctuations (Fugate and Fry, 1956), particularly pupillary hippus (an involuntary spasm of the pupil) (Fry and King, 1975; Hopkinson, 1956) but later work showed little correlation with pupil size fluctuations and discomfort glare (Howarth et al., 1993). Electromyographic techniques (EMG) have also been employed, which examined facial muscle activity under conditions of discomfort (Berman et al., 1994; Murray et al., 2002). Determining whether visual discomfort is associated with particular facial muscle activity, distraction (Lynes, 1977) or with certain eye-movement behavior (Vos, 2003b) may lead to better detection or characterization of discomfort glare, but it provides little information as to the cause.

* Corresponding author.

E-mail address: gary.bargary.1@city.ac.uk (G. Bargary).

Recently, evidence has emerged that visual scenes departing from natural image statistics result in higher visual discomfort (Fernandez and Wilkins, 2008; Juricevic et al., 2010), which is thought to be caused by hyperexcitability of neurons in response to unnatural stimuli (Juricevic et al., 2010). In agreement with this hypothesis, it has been found that discomfort ratings of different colored gratings correlate positively with the cortical haemodynamic response, as measured with near infrared spectroscopy (Haigh et al., 2013). High contrast, achromatic or colored gratings also cause a constriction of the pupil which has been linked to the level of cortical activity generated since these pupil response components remain even in the absence of damaged subcortical projections that abolish the light reflex response (Barbur, 2004; Wilhelm et al., 2002). In the case of discomfort glare where high luminance sources are often used, hyperexcitability or saturation of a set of neurons is likely to occur; and as suggested by Wilkins and others (Haigh et al., 2013; Wilkins et al., 1984), the discomfort may be a homeostatic response, the purpose of which is to decrease the metabolic load. The current work employs glare sources with controlled levels of retinal illuminance and fMRI, in order to test whether discomfort glare is associated with hyperexcitability in different regions of the cortex.

Any study that involves judgements of discomfort glare needs to address the large inter-individual variation (Luckiesh and Guth, 1949; Saur, 1969; Stone and Harker, 1973). This study makes use of this variation by examining fMRI bold responses of two sets of participants who differed in their sensitivity to discomfort glare, i.e. low and high glare sensitivity. Each participant was presented with three different light levels that caused low, medium and high levels of glare, as defined by examining the distribution of discomfort glare thresholds in the full set of participants. Pupil diameter was also measured, enabling specification of the stimulus in terms of retinal illuminance, a parameter that relates directly to photoreceptor saturation. The primary comparisons made were between the two sets of participants at each light level tested, with the aim of identifying cortical regions where hyperactivity may occur in glare-sensitive individuals and characterizing how activity varies with glare intensity in such regions.

2. Methods

2.1. Participants

Twenty-eight participants (mean age=39.96, SD=16.25, 13 females) took part in this experiment. All reported normal or corrected to normal vision and were screened accordingly to standard MRI exclusion criteria. Furthermore, they reported no history of psychiatric or neurological disorders, and no current use

of psychoactive medication. Written informed consent was obtained prior to participation. The experimental procedure was in accord with the Declaration of Helsinki and was approved by the appropriate local ethics committees.

2.2. Overall design

Prior to carrying out the fMRI experiment, each participant had his/her threshold for discomfort glare assessed behaviorally. The participants were then divided into two groups of equal size based on their ranked sensitivity to discomfort glare. Each participant then partook in an fMRI experiment under three different light levels that normally generate low, medium and high levels of glare. The corresponding retinal illuminances were 3.95, 4.95 and 5.95 log Trolands, respectively. These light levels were chosen to be one log unit apart; both below and above the mean discomfort-glare threshold obtained from the initial behavioural assessment; this initial assessment was carried out on a larger population of 41 participants and a smaller subset of these participants (28) went on to do the fMRI experiment. Specification of the stimulus in terms of retinal illuminance ensures that, in spite of differences in pupil size, the light per unit area on the retina is approximately constant for each participant for a given light level.

2.3. Stimuli and apparatus

In both the preliminary behavioral experiment and the fMRI experiment glare was introduced using four Perkin Elmer LED units mounted on a circular device that surrounded a visual display, Fig. 1. The complete LED apparatus was constructed from MRI compatible materials. The LEDs were positioned at four different locations (0°, 90°, 180°, and 270°) at an eccentricity of 12° of visual angle. In the behavioral experiment the visual display used was an LCD monitor (19" NEC SpectraView 1990SXi). The visual display and LED lights were calibrated with a spectroradiometer (Konica Minolta, CS-2000), and a luminance meter (LMT 1009). The chromaticity of the LEDs and visual display were close to D_{65} : ($x=0.305$, $y=0.323$, CIE 1931 chromaticity space). The output of the LEDs was calibrated by measuring the illuminance generated in the plane of the pupil; the ambient background luminance surrounding each LED was ~ 5 cd/m². Simultaneous with the onset of the LED lights, stimuli were presented in the center of the visual display. The stimuli consisted of a fixation cross (subtending 1°), which was followed by a Landolt C with a diameter of 20 min of arc. The Landolt C appeared 0.75–1.5 s after the disappearance of the fixation-cross; each Landolt C was presented at a fixed Weber contrast of 300% with the Landolt ring gap in one of four randomly selected orientations. The background luminance of the visual display was 24 cd/m². The participant viewed the stimulus

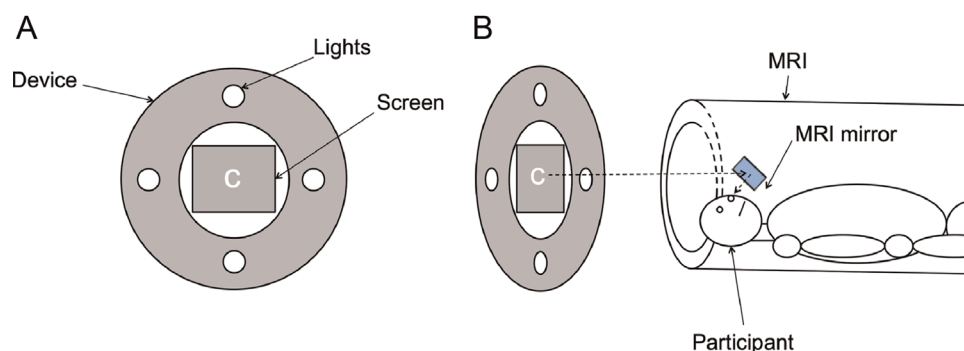


Fig. 1. Apparatus. Panel A. Device used to produce discomfort glare. Four MRI compatible LED light sources were mounted on a circular device surrounding a rear-projection screen onto which Landolt C stimuli could be projected. Panel B. The device was placed at the end of the MRI bore and the participant viewed the stimulus through a mirror mounted on the head coil.

apparatus from a distance of 1.5 m using a chin rest fitted with pulsed infrared illumination and a video camera operating at 50 Hz. Pupil diameter was recorded every 20 ms and was used to calculate retinal illuminance.

In the fMRI experiment, computer-generated visual stimuli were projected by an LCD projector onto a small rear-projection screen at the end of the scanner bore. The projection screen was mounted in the center of the LED apparatus (in the same position as that occupied by the visual display in the behavioral experiment). Both the projection screen and LEDs were viewed via a mirror mounted on the head coil; the viewing distance was 1.5 m. The screen stimuli were identical to those used in the behavioral experiment. All stimuli were controlled using Matlab programs (The Mathworks, Inc.). Eye images were continuously obtained with an infrared video camera positioned close to the eye (NordicNeuroLab, Norway). Pupil recordings were used at the start of the fMRI experiment to set the light level to one of three different retinal illuminance levels: 3.95, 4.95 and 5.95 log Trolands for the low, medium and high glare levels, respectively.

2.4. Procedure

2.4.1. Behavioral

Discomfort glare thresholds were obtained by the method of adjustment. Each participant was instructed to maintain fixation on the center of the LCD monitor and to adjust the brightness of the LEDs until discomfort was experienced; the adjustment was carried out using button control and each step was a change of 1.5 lx. A number of practice trials were carried out beforehand to ensure the participant understood the task and the judgement s/he was required to make. Once practice was completed, 10 trials were carried out; the starting illuminance was varied pseudorandomly on each trial. On each of the ten trials once the participant had chosen the appropriate brightness level, which could take approximately one to two minutes, the brightness was fixed and the participant had to carry out five Landolt C orientation discriminations, in sequence. This sequence lasted 15 s and was included to give the participant a stimulus setup that would be more representative of what s/he would experience in the fMRI scanner. Pupil diameter was measured throughout and the discomfort glare threshold for each trial was recorded in log Trolands. A mean threshold from the last 8 out of 10 trials (in log Trolands) provided a measure of the participant's discomfort glare threshold.

Averaging was carried out in log units as discomfort glare thresholds measured in log Trolands are approximately normally distributed.

2.4.2. Neuroimaging

A block design was employed. Each scan run started with the white central fixation cross being presented on the black background for 15 s while the LEDs were turned off. Then the LEDs turned on and their luminosity was ramped up using a cosine ramp over a period of one second until they reached one of the three light intensities (ON phase). The ON phase lasted 15 s, after which the lights were ramped off over one second and remained off (OFF phase) for a further 15 s. Each of the three luminance levels was repeated three times in a random order within the same run, giving nine ON blocks per run. An additional OFF phase lasting 15 s was introduced near the middle of each run, in order to de-phase physiological noise that might be present at frequencies close to the block repetition frequency. In half the runs, the additional OFF phase was introduced after the fourth stimulus block, while in the other half it was introduced after the fifth run. The whole session consisted of eight runs.

Throughout each run, the participant continuously performed a Landolt C task. Thus, modulations in BOLD response reflected the luminance modulations described above and not task-related activity, which was approximately constant. The task was intended to maximize the extent to which BOLD responses to luminance encapsulated glare effects as well as simple sensory responses to light. The participant initially fixated the central fixation cross. After 15 s, the cross disappeared and after a variable delay of 250–750 ms a Landolt C appeared in the center of the screen in one of the four orientations, and stayed on the screen for 200 ms. A series of four letters was presented, interleaved by a variable time between 0.75 and 1.25 s after the participant's response; the participant was given 2.5 s to respond, after this time without response the trial was categorized as incorrect and a miss. The task of the participant was to indicate the orientation of each Landolt C by pressing one of four buttons (Fig. 2). After a period of two seconds with no letters, another sequence of four letters was presented, and so on. Targets were grouped only for consistency with the psychophysical experiments and presentation was regarded as continuous for the purpose of the fMRI design.

In order to specify the light level in terms of retinal illuminance, prior to the fMRI scan (but while the participant was in the

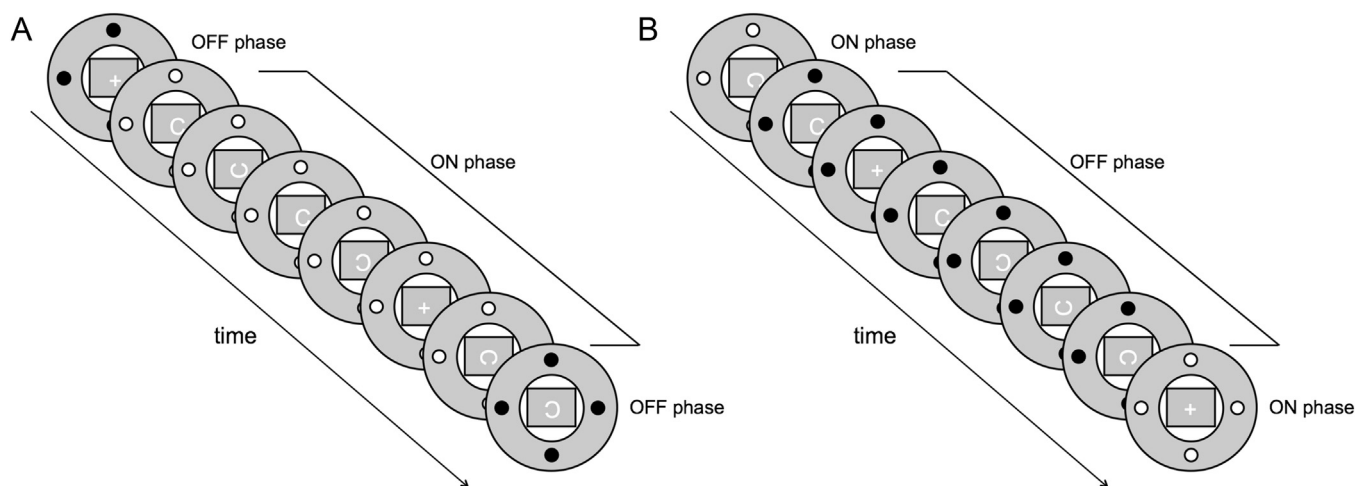


Fig. 2. Procedure. Each run started with a fixation-cross shown in the center of the screen. After 15 s, the first sequence of four Landolt Cs was shown on the screen. Each Landolt C could be in one of four orientations and was separated from the next one by a variable time spanning from 0.75 to 1.25 s after the participant's response. The participant responded by pressing one of four buttons, which indicated the orientation of each Landolt C. After this sequence, a fixation cross was shown for 2 s, after which another sequence of four Landolt C presentations began. While the participant was attending the Landolt C task, s/he was exposed to lights for 15 s (ON phase, panel A), followed again by a rest phase with no lights (OFF phase, panel B).

MRI scanner), the pupil diameter of each participant was measured while simultaneously (in near to real time) changing the light level to equate to one of the three retinal illuminances. This procedure was maintained until the average retinal illuminance for a five second time-window was within 0.05 log units of the required value. The illuminance level at the plane of the pupil for this retinal illuminance was then chosen and used for the entire fMRI experiment. This was carried out for each of the three retinal illuminance levels: low glare, medium glare and high glare.

2.5. Data acquisition

MRI images were obtained with a 3-Tesla Siemens Magnetom TIM Trio scanner and a standard Siemens 32-channel array head coil. Anatomical (T1-weighted) images were obtained at the beginning of each scanning session (MP-RAGE, 160 axial slices, in plane resolution 256×256 , 1 mm isotropic voxels, TR=1830 ms, TE=4.43 ms, flip angle=11°, bandwidth=130 Hz/pixels). This was followed by eight functional scanning runs. The functional data were acquired with a gradient echo, echoplanar sequence (TR=2500 ms, 36 slices, interleaved acquisition order, 3 mm isotropic voxels, FOV = 192×192 mm, flip angle=85°, TE=31 ms, bandwidth=752 Hz/pixel). Each scan consisted of 120 acquisition volumes, and lasted 5 min.

2.6. Data analysis

All the preprocessing and analyses were performed with BrainVoyager QX (version 2.3, Brain Innovation, Inc, The Netherlands). The first 3 volumes of each functional run were discarded in order to avoid T1-saturation artefacts. The remaining functional data were corrected for slice timing (using trilinear interpolation) and were filtered with a high pass filter of 3 cycles/scan (approx. 0.01 Hz). Correction for 3D head motion was applied using rigid body transformation and trilinear interpolation. To do this, the first functional volume of the first scan run for each participant was used as a reference to which all the subsequent functional images from both the same run and the following runs were aligned. The same functional image was used for coregistering functional data with anatomical data. Both anatomical and functional data were spatially normalized across participants by transforming each data set to standard Talairach space (Talairach & Tournoux, 1988). Spatial smoothing was achieved by applying a kernel of 4.5 mm full-width at maximum Gaussian filter (FWHM).

All data were analyzed with standard methods. Each event type was modeled by convolving the block timing with a canonical

hemodynamic impulse response function ($\delta=2.5$, $\tau=1.25$, Boynton, Engel, Glover, & Heeger, 1996). A separate model was generated for each block type (luminance level). The resulting reference time-courses were used to fit the percentage-signal-change (PSC) transformed time course of each voxel within the whole brain by means of a random-effects (RFX) analysis. The output of the first-level analysis general linear model (GLM) provided beta values representing the mean response estimates at each voxel for each subject separately. These were then assessed using t and F statistics at the second level.

3. Results

3.1. Behavioral

Discomfort glare thresholds ranged in value from 3.99 to 6.13 log Trolands, with a mean of 5.06 (sd=0.61). Performance on the Landolt C gap orientation task in the fMRI experiment, across all conditions (no glare, low, medium or high glare), had a mean percentage correct of 94.12 (sd=7.69); the median value was 97.68. The means were similar for each condition considered separately, a repeated measures anova revealed no significant difference, $F(3, 72)=0.229$, $p=0.876$. Three participants' behavioral results had to be excluded owing to equipment failure.

3.2. Neuroimaging

3.2.1. Effect of light on sensitive and less sensitive participants

The overall difference between the two participant groups was assessed by pooling the three levels of light intensity and contrasting the first group (sensitive to glare) with the second group (less sensitive to glare) (i.e., $G1(L1,L2,L3)-G2(L1,L2,L3)$). This comparison revealed that the group sensitive to glare showed increased neural activity in bilateral lingual gyri (left: $t_{(27)}=6.76$, $p_{(corr)} < 0.01$; right: $t_{(27)}=6.47$, $p_{(corr)} < 0.01$), bilateral cuneus (left: $t_{(27)}=7.01$, $p_{(corr)} < 0.01$; right: $t_{(27)}=6.31$, $p_{(corr)} < 0.01$) and in the superior parietal lobule (left: $t_{(27)}=6.43$, $p_{(corr)} < 0.01$; right: $t_{(27)}=6.36$, $p_{(corr)} < 0.01$) (Fig. 3). Table 1 reports the locations of the regions found. The t -values quoted are the peak values for each region and the p values are corrected for multiple comparisons.

3.2.2. Cortical responses for low, medium and high luminosity

The difference between the two groups was assessed for each level of luminosity separately with three further contrasts (first contrast: $G1(L1)-G2(L1)$, second contrast: $G1(L2)-G2(L2)$, third

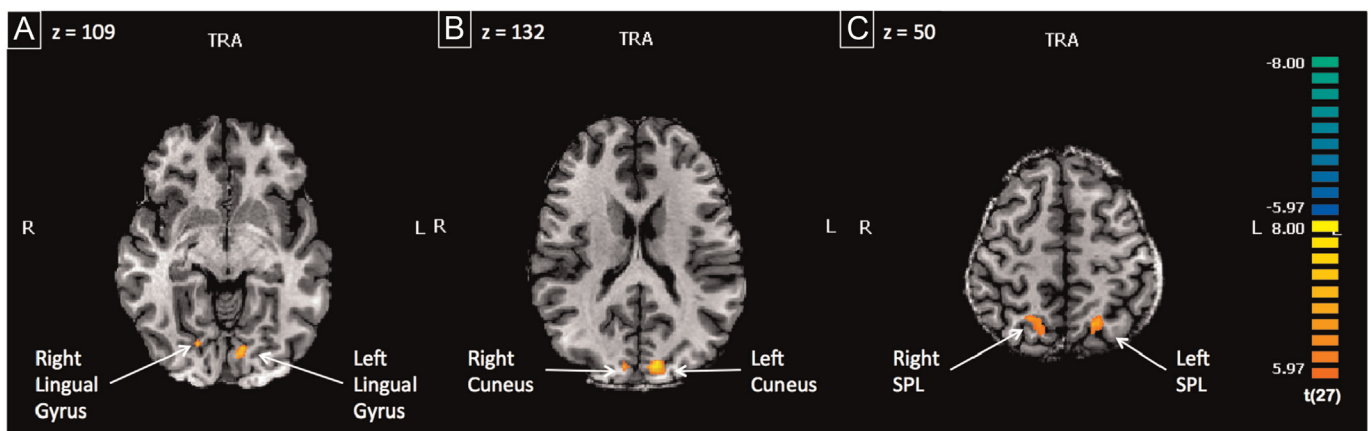


Fig. 3. Responses in bilateral lingual gyrus (A) and bilateral cuneus (B) and superior parietal lobe (C) resulting from the comparison of the three levels of luminosity combined together (L1, L2, and L3) contrasted between the group sensitive (G1) and the group insensitive to glare (G2). Brain slices are in radiological convention. All slice locations identified are in Talairach coordinates.

Table 1
Brain regions showing a significant difference in BOLD response for the between groups contrast [G1(L1,L2,L3) > G2(L1,L2,L3)]. This contrast represents the difference in the response to luminance (L1, L2, and L3) between the group sensitive to glare (G1) and the group insensitive to glare (G2). Statistical threshold was corrected for multiple comparisons.

Anatomical region	Hem	Cluster size voxel	Talairach coordinats mean ± SD			t value t(27)	Mean p value (Bonf. corrected)
			X	y	z		
Cuneus	R	88	6.97 ± 1.23	−85.48 ± 1.39	17.89 ± 1.32	6.3142	< 0.001
Cuneus	L	917	−12.36 ± 2.92	−86.01 ± 2.19	22.42 ± 4.18	7.0082	< 0.001
Lingual	R	79	16.68 ± 1.11	−71.15 ± 1.52	−2.85 ± 1.59	6.4736	< 0.001
Lingual	L	234	−10.23 ± 2.44	−75.97 ± 2.15	−5.02 ± 1.29	6.7649	< 0.001
SPL	R	432	16.20 ± 3.24	−59.61 ± 3.19	51.21 ± 1.59	6.4736	< 0.001
SPL	L	398	−20.85 ± 1.93	−59.71 ± 3.09	48.56 ± 1.60	6.7649	< 0.001

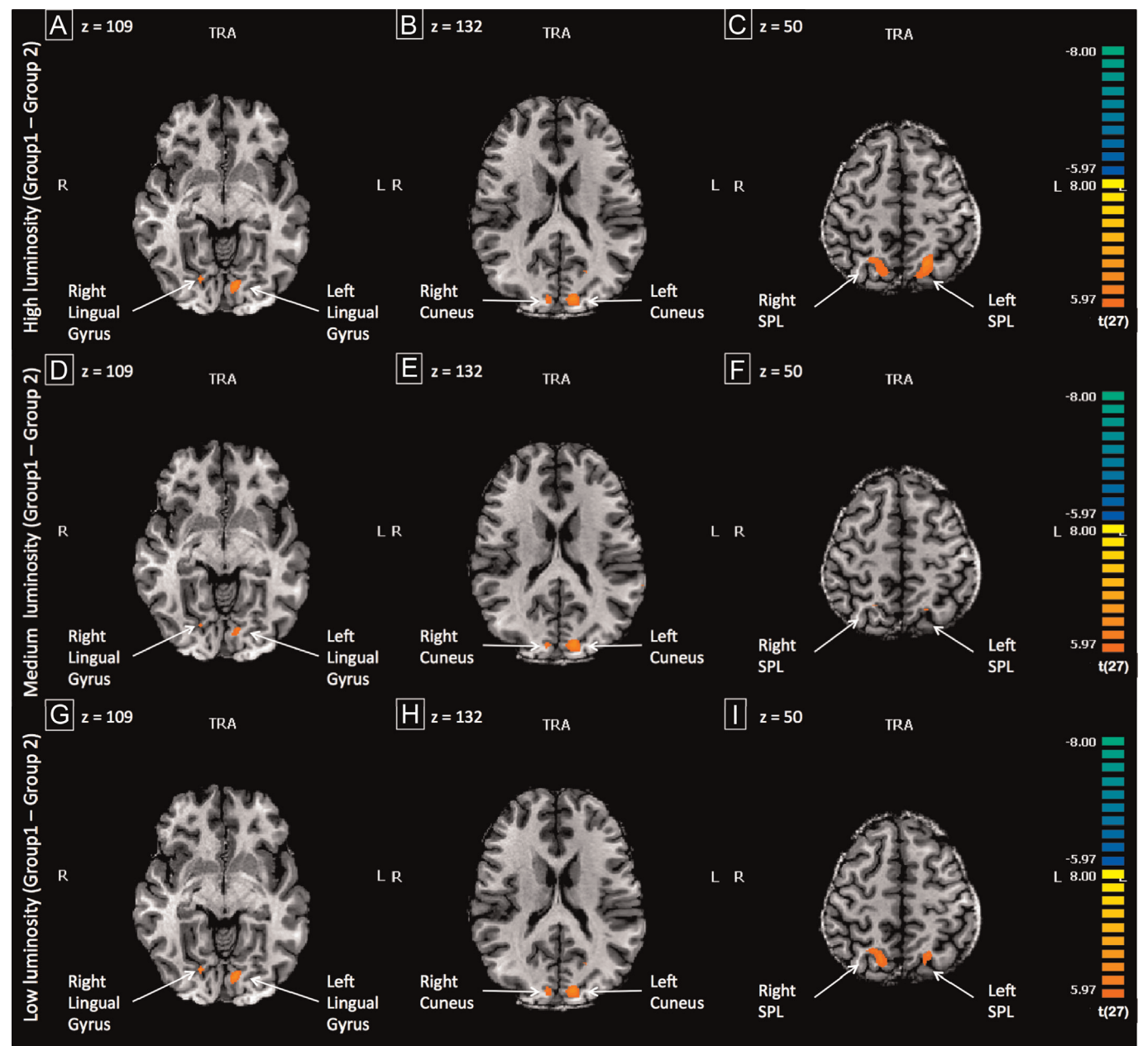


Fig. 4. Responses in bilateral lingual gyrus (A,D,G), bilateral cuneus (B,E,H) and superior parietal lobule (C,F,I) for each of the three levels of luminance contrasted between the groups sensitive (G1) and the insensitive (G2) to glare. A–C: responses to High luminosity [G1(L1)–G2(L1)]. D–F: responses to middle luminosity [G1(L2)–G2(L2)]. G–I: response to low luminosity [G1(L3)–G2(L3)]. Brain slices are in radiological convention. All slice locations identified are in Talairach coordinates.

Table 2

Brain regions showing significant difference in BOLD response for the between groups contrasts G1(L1) > G2(L1) (upper panel), G1(L2) > G2(L2) (middle panel) and G1(L3) > G2(L3) (lower panel). Statistical threshold was corrected for False Discovery Rate (FDR(q)=0.05).

Light intensity	Anatomical region	Hem	Cluster size voxel	Talairach coordinates (mean \pm SD)			<i>t</i> Value <i>t</i> (27)	Mean <i>p</i> value (Bonf. corrected)
				X	y	z		
High	Cuneus	R	195	6.49 \pm 1.20	−86.89 \pm 2.03	19.94 \pm 2.80	3.1985	ns (< 0.002 unc)
	Cuneus	L	789	−12.10 \pm 2.75	−86.20 \pm 3.51	21.83 \pm 1.46	3.8432	< 0.05
	Lingual	R	148	17.03 \pm 1.34	−72.33 \pm 2.27	−1.05 \pm 2.82	3.6532	< 0.05
	Lingual	L	328	−9.90 \pm 2.65	−76.34 \pm 2.38	−5.05 \pm 1.46	3.4842	ns (< 0.001 unc)
	SPL	R	687	−15.62 \pm 3.66	−60.45 \pm 4.12	50.51 \pm 2.14	3.7678	< 0.05
	SPL	L	1588	−19.89 \pm 3.05	−76.34 \pm 2.38	−5.05 \pm 1.46	3.9080	< 0.05
Medium	Cuneus	R	90	6.66 \pm 1.38	−85.51 \pm 1.27	17.52 \pm 1.46	3.4066	ns (< 0.001 unc)
	Cuneus	L	933	−12.72 \pm 2.80	−85.88 \pm 2.22	22.41 \pm 4.21	3.8044	0.0003
	Lingual	R	22	16.86 \pm 0.76	−71.05 \pm 0.88	−3.09 \pm 0.79	4.1654	< 0.05
	Lingual	L	169	−11.02 \pm 2.42	−75.64 \pm 1.77	−5.22 \pm 1.22	3.7146	< 0.05
	SPL	R	169	−16.58 \pm 2.09	−57.65 \pm 1.79	−50.90 \pm 0.39	4.1656	< 0.05
	SPL	L	169	−20.59 \pm 1.11	−58.41 \pm 1.17	48.69 \pm 0.88	4.7300	< 0.05
Low	Cuneus	R	27	7.81 \pm 0.72	−85.56 \pm 1.20	18.04 \pm 0.74	3.6923	< 0.05
	Cuneus	L	594	−11.56 \pm 2.57	−86.63 \pm 1.96	21.11 \pm 3.11	3.9803	< 0.05
	Lingual	R	104	17.21 \pm 1.33	−72.22 \pm 2.50	−1.43 \pm 3.25	3.7979	< 0.05
	Lingual	L	134	−9.85 \pm 2.05	−75.96 \pm 1.84	−4.77 \pm 1.13	3.8450	< 0.05
	SPL	R	134	−15.61 \pm 3.29	−61.06 \pm 3.94	−50.65 \pm 3.94	3.7211	< 0.05
	SPL	L	134	−3.94 \pm 1.78	−60.99 \pm 2.78	−48.83 \pm 1.41	4.3650	< 0.05

contrast: G1(L3)–G2(L3)). These contrasts confirmed that the group sensitive to glare showed significantly greater activity in bilateral cuneus, bilateral lingual gyri and bilateral superior parietal sulci for each luminance considered separately. Fig. 4 shows the results from each contrast, while the coordinates in Talairach space, together with cluster size and statistical values, are reported in Table 2. As an additional test for differential effects of participant group at different luminance levels, a 2-way ANOVA (groups \times luminance) was conducted based on the beta values from the first-level GLM analysis. This showed no significant interaction between the two factors in any brain region. Thus, sensitive participants have greater responses to light than less sensitive participants but this difference is not dependent on how this level of light relates to each participant's discomfort glare threshold i.e. whether the participant is in discomfort or not.

4. Discussion

Empirical observations make it possible to predict with reasonable accuracy how uncomfortable a given lighting installation is likely to be (CIE, 1995; Vos, 1999), yet we understand very little, from a physiological perspective, about why these predictions hold true. Evidence exists that hyperexcitability or saturation of a set of neurons is involved in visual discomfort when viewing uncomfortable standard contrast images (Haigh et al., 2013), but it has yet to be established if it plays a role when a subject experiences discomfort glare as a result of viewing bright lights. This study compared neural responses between two groups of participants that differ in their sensitivity to discomfort glare. We predicted that, in certain cortical areas, the group with high sensitivity to glare would show increased neural activity when compared with the low sensitivity group. This was indeed found to be case at each of the three light levels examined. The increased response was localized bilaterally in the brain, specifically in the cuneus, the lingual gyri and the superior parietal lobules (SPL).

The finding that these cortical areas were more active in the high sensitivity group at each light level, even when the light level was below each participant's discomfort glare threshold, suggests that these areas are not involved specifically in the signaling of

visual discomfort; rather, they may represent a standard neuronal response to high contrast light-sources in the visual field. The magnitude of the neuronal response, however, is positively correlated with individuals' sensitivity to discomfort glare. This suggests that varying degrees of neuronal hyperexcitability may underlie the differences in discomfort glare thresholds between the high and low sensitivity groups.

Neuronal hyperexcitability has already been implicated in a number of phenomena related to discomfort glare, such as: visual discomfort (Haigh et al., 2013; Juricevic et al., 2010), photophobia (Boulloche et al., 2010; Denuelle et al., 2011) and light-induced migraine (Coutts et al., 2012; Hougaard et al., 2014). For example, using positron emission topography (PET), Boulloche and colleagues (Boulloche et al., 2010) found increased bilateral activity in the visual cortex (specifically the cuneus, lingual gyrus and posterior cingulate cortex) in migraineurs with photophobia at multiple light levels. Similarly, Huang and colleagues (Huang et al., 2003) present fMRI evidence for hyperexcitability of the occipital lobe in migraineurs with aura. More recently, they showed that wearing certain tinted lenses (Huang et al., 2011), which reduce migraine symptoms, also reduces cortical hyperexcitability. A study using near infrared spectroscopy found that the cortical haemodynamic response correlated positively with discomfort ratings to different colored gratings (Haigh et al., 2013). There is a wide network of brain areas involved in visual discomfort, photophobia and photo-induced pain responses, both cortical (Boulloche et al., 2010; Denuelle et al., 2011) and subcortical (Moulton et al., 2009; Nosedá et al., 2010; Okamoto et al., 2010); however, hyperexcitability may need to be present only at the initial stages of this processing hierarchy.

Hyperexcitability is thought to relate to visual discomfort through a homeostatic process (Wilkins et al., 1984). Cortical areas that are hyperactive have a higher metabolic demand and it is suggested that the discomfort itself is a homeostatic response, which may initiate a behavior that will reduce the metabolic load (Haigh et al., 2013; Wilkins et al., 1984). The metabolic demands of neuronal signaling are substantial; indeed it has been estimated that, given the energy requirements of action potentials and synaptic signal transmission, only a small fraction of the cerebral cortex can be active at any given time (Attwell and Laughlin, 2001;

Howarth et al., 2012). High luminance LED light sources, as used in this study, are likely to cause saturation or hyperexcitability of a certain set of neurons. The degree to which an individual's low-level visual areas are susceptible to hyperexcitability may explain some of the inter-individual variation in discomfort glare thresholds (Luckiesh and Guth, 1949; Saur, 1969; Stone and Harker, 1973), although some of this variance will be attributable to differences in individuals' subjective criteria for discomfort. However, it has yet to be determined why individuals sensitive to discomfort glare exhibit greater hyperexcitability. One possibility is that the neurons involved are intrinsically more excitable; another is that there is a lack of sufficient neural inhibition. Also, there may be differences in the shape of the haemodynamic response function between individuals, such as in the onset or offset (Coutts et al., 2012).

Given the claim that discomfort glare arises ultimately from saturation or hyperexcitability of low-level visual areas, it may be of interest to lighting engineers to consider the physiological properties of the early visual system. In central vision, for example, the physiological properties of photoreceptors and the ON-OFF center-surround organization of ganglion cells bias responses towards luminance-defined edges, whereas responses in the periphery may be more biased towards light flux, as there is summing of responses over larger areas of the visual field. Indeed, in previous work (Bargary et al., 2015), a model based solely on saturation of visual transduction mechanisms predicted discomfort glare thresholds for centrally viewed light sources.

5. Conclusions

This study compared neuronal activity in two groups of individuals who differ in their sensitivity to discomfort glare. We found that the group that was more sensitive to discomfort glare had an increased neuronal response in certain low-level visual areas. This increased response was independent both of the light level used and the presence or absence of discomfort glare. The results suggest that sensitivity to discomfort glare is determined, at least in some degree, by how excitability ones visual neurons are.

Acknowledgements

The authors would like to thank Navaz Davoudian and Edward Barratt from University College London (UCL) for their collaboration and recruitment of participants. We also like to thank Arthur Collyer and Alister Harlow for support with the construction of equipment and technical support. This research was funded by the Engineering and Physical Sciences Research Council (EPSRC) (grant reference numbers; EP/G044538/1 and EP/I003940/1).

References

Attwell, D., Laughlin, S.B., 2001. An energy budget for signaling in the grey matter of the brain. *J. Cereb. Blood Flow Metab.* 21 (10), 1133–1145. <http://dx.doi.org/10.1097/00004647-200110000-00001>.

Barbur, J., 2004. Learning from the pupil: studies of basic mechanisms and clinical applications. In: Chalupa, L.M., Werner, J.S. (Eds.), *The Visual Neurosciences*. MIT Press, Cambridge, Massachusetts, pp. 641–656.

Bargary, G., Jia, Y., Barbur, J.L., 2015. Mechanisms for discomfort glare in central vision. *Investig. Ophthalmol. Vis. Sci.* 56 (1), 464–471. <http://dx.doi.org/10.1167/iov.14-15707>.

Berman, S.M., Bullimore, M.A., Jacobs, R.J., Bailey, I.L., Ghandi, N., 1994. An objective measure of discomfort glare. *J. Illum. Eng. Soc.* 23 (2), 40–49.

Bouloche, N., Denuelle, M., Payoux, P., Fabre, N., Trotter, Y., Géraud, G., 2010. Photophobia

in migraine: an interictal PET study of cortical hyperexcitability and its modulation by pain. *J. Neurol. Neurosurg. Psychiatry* 81 (9), 978–984. <http://dx.doi.org/10.1136/jnnp.2009.190223>.

CIE, 1995. Discomfort Glare in Interior Lighting, CIE #117.

Coutts, L.V., Cooper, C.E., Elwell, C.E., Wilkins, A.J., 2012. Time course of the haemodynamic response to visual stimulation in migraine, measured using near-infrared spectroscopy. *Cephalalgia* 32 (8), 621–629. <http://dx.doi.org/10.1177/0333102412444474>.

Denuelle, M., Bouloche, N., Payoux, P., Fabre, N., Trotter, Y., Géraud, G., 2011. A PET study of photophobia during spontaneous migraine attacks. *Neurology* 76 (3), 213–218. <http://dx.doi.org/10.1212/WNL.0b013e3182074a57>.

Fernandez, D., Wilkins, A.J., 2008. Uncomfortable images in art and nature. *Perception* 37 (7), 1098–1113.

Fry, G.A., King, V.M., 1975. The Pupillary Response and Discomfort Glare. *J. Illum. Eng. Soc.* 4 (4), 307–324. <http://dx.doi.org/10.1080/00994480.1975.10748533>.

Fugate, J.M., Fry, G.A., 1956. Relation of changes in pupil size to visual discomfort. *Illum. Eng.* 51 (7), 537–549.

Haigh, S.M., Barningham, L., Berntsen, M., Coutts, L.V., Hobbs, E.S.T., Irabor, J., Wilkins, A.J., 2013. Discomfort and the cortical haemodynamic response to coloured gratings. *Vis. Res.* 89, 47–53. <http://dx.doi.org/10.1016/j.visres.2013.07.003>.

Holladay, L.L., 1926. The fundamentals of glare and visibility. *J. Opt. Soc. Am.* 12 (4), 271–319. <http://dx.doi.org/10.1364/JOSA.12.000271>.

Hopkinson, R.G., 1956. Glare discomfort and pupil diameter. *J. Opt. Soc. Am.* 46 (8), 649–656.

Hopkinson, R.G., 1957. Evaluation of glare. *Illum. Eng.* 52, 305–316.

Hougaard, A., Amin, F.M., Hoffmann, M.B., Rostrup, E., Larsson, H.B.W., Asghar, M.S., Ashina, M., 2014. Interhemispheric differences of fMRI responses to visual stimuli in patients with side-fixed migraine aura. *Hum. Brain Map.* 35 (6), 2714–2723. <http://dx.doi.org/10.1002/hbm.22361>.

Howarth, C., Gleeson, P., Attwell, D., 2012. Updated energy budgets for neural computation in the neocortex and cerebellum. *J. Cereb. Blood Flow Metab.* 32 (7), 1222–1232. <http://dx.doi.org/10.1038/jcbfm.2012.35>.

Howarth, P.A., Heron, G., Greenhouse, D.S., Bailey, I.L., Berman, S.M., 1993. Discomfort from glare: the role of pupillary hippus. *Light. Res. Technol.* 25, 37–42. <http://dx.doi.org/10.1177/096032719302500106>.

Huang, J., Cooper, T.G., Satana, B., Kaufman, D.I., Cao, Y., 2003. Visual distortion provoked by a stimulus in migraine associated with hyperneuronal activity. *Headache* 43 (6), 664–671.

Huang, J., Zong, X., Wilkins, A., Jenkins, B., Bzokki, A., Cao, Y., 2011. fMRI evidence that precision ophthalmic tints reduce cortical hyperactivation in migraine. *Cephalalgia* 31 (8), 925–936. <http://dx.doi.org/10.1177/0333102411409076>.

Juricevic, I., Land, L., Wilkins, A., Webster, M.A., 2010. Visual discomfort and natural image statistics. *Perception* 39 (7), 884–899.

Luckiesh, M., Guth, S.K., 1949. Brightness in visual field at borderline between comfort and discomfort. *Illum. Eng.* 44 (11), 650–670.

Luckiesh, M., Holladay, L.L., 1925. Glare and visibility. *Trans. Illum. Eng. Soc.* 20 (3), 221–252.

Lynes, J.A., 1977. Discomfort glare and visual distraction. *Light. Res. Technol.* 9 (1), 51–52. <http://dx.doi.org/10.1177/096032717700900106>.

Moulton, E.A., Becerra, L., Borsook, D., 2009. An fMRI case report of photophobia: activation of the trigeminal nociceptive pathway. *Pain* 145 (3), 358–363. <http://dx.doi.org/10.1016/j.pain.2009.07.018>.

Murray, I., Plainis, S., Carden, D., 2002. The ocular stress monitor: a new device for measuring discomfort glare. *Light. Res. Technol.* 34 (3), 231–242. <http://dx.doi.org/10.1191/1365782802lt046oa>.

Nosedá, R., Kainz, V., Jakubowski, M., Gooley, J.J., Saper, C.B., Digre, K., Burstein, R., 2010. A neural mechanism for exacerbation of headache by light. *Nat. Neurosci.* 13 (2), 239–245. <http://dx.doi.org/10.1038/nn.2475>.

Okamoto, K., Tashiro, A., Chang, Z., Bereiter, D.A., 2010. Bright light activates a trigeminal nociceptive pathway. *Pain* 149 (2), 235–242. <http://dx.doi.org/10.1016/j.pain.2010.02.004>.

Saur, R.L., 1969. Influence of physiological factors on discomfort glare level. *Am. J. Optom. Arch. Am. Acad. Optom.* 46 (5), 352–357.

Stiles, W.S., 1929a. The effect of glare on the brightness difference threshold. *Proc. R. Soc. B: Biol. Sci.* 104 (731), 322–351. <http://dx.doi.org/10.1098/rspb.1929.0012>.

Stiles, W.S., 1929b. The nature and effects of glare. *Illum. Eng.* 22, 304–312.

Stiles, W.S., 1929c. The scattering theory of the effect of glare on the brightness difference threshold. *Proc. R. Soc. Lond. Ser. B, Contain. Pap. Biol. Charact.* 105, 131–146.

Stone, P.T., Harker, S.D.P., 1973. Individual and group differences in discomfort glare responses. *Light. Res. Technol.* 5, 41–49.

Van den Berg, T.J.T.P., Franssen, L., Kruijt, B., Coppens, J.E., 2013. History of ocular stray-light measurement: a review. *Z. Med. Phys.* 23 (1), 6–20. <http://dx.doi.org/10.1016/j.zemedi.2012.10.009>.

Vermeulen, D., de Boer, J.B., 1952. On the admissible brightness of lighting fixtures. *Appl. Sci. Res. Sect. B* 2 (1), 85–107. <http://dx.doi.org/10.1007/BF02919762>.

Vos, J.J., 1999. Glare today in historical perspective: towards a new CIE glare observer and a new glare nomenclature. In: *Proceedings of CIE 24th Session, Warsaw, I-1*, pp. 38–42.

Vos, J.J., 2003a. On the cause of disability glare and its dependence on glare angle, age and ocular pigmentation. *Clin. Exp. Optom.: J. Aus. Optom. Assoc.* 86 (6), 363–370.

Vos, J.J., 2003b. Reflections on glare. *Light. Res. Technol.* 35, 163–176. <http://dx.doi.org/10.1191/1477153503li083oa>.

Wilhelm, B.J., Wilhelm, H., Moro, S., Barbur, J.L., 2002. Pupil response components: studies in patients with Parinaud's syndrome. *Brain: J. Neurol.* 125 (Pt 10), 2296–2307.

Wilkins, A., Nimmo-Smith, I., Tait, A., McManus, C., Della Sala, S., Tilley, A., Scott, S., 1984. A neurological basis for visual discomfort. *Brain: J. Neurol.* 107 (Pt 4), 989–1017.